

# BER Reduction for DMT-ADSL Based on DMWT

Salih Mohammed Salih

*Electrical Engineering Department, University of Anbar, Al-Anbar, Iraq  
dr\_salih\_moh@yahoo.com*

---

**Özet.** Ayrık çoklu-tonlamalı (DMT) modülasyon, asimetrik dijital abone hatlarında kullanılan bir dik frekans bölmeli çoğullama (OFDM) modülasyon modelidir ve diğer hızlı geniş bantlı erişim sistemleri için de önerilmektedir. DMT-ADSL'in bit hata oranını (BER) geliştirmek için bir ayrık çoklu-dalgacık dönüşüm (DMWT) modeli önerilmiştir. Standart model ve önerilen modelin performansları toplanabilir beyaz Gauss gürültülü (AWGN) kanal etkisi altında Matlab yazılımı kullanılarak simule edilmiştir. Ayrıca, rasgele darbe bit konum gürültü etkisi de simülasyonumuza alınmıştır. Simülasyon sonuçları, DMWT tekniğine dayanan modelin BER açısından standart modelden daha yüksek seviyede performans gösterdiğini ortaya koymuştur.<sup>†</sup>

**Anahtar Kelimeler.** DMT, ADSL, AWGN, FFT, DMWT, darbe gürültüsü.

**Abstract.** Discrete multi-tone (DMT) modulation is an orthogonal frequency division multiplexing (OFDM) based modulation scheme used in asymmetrical digital subscriber line (ADSL) and proposed for various other high-speed broadband access systems. To enhance the bit error rate (BER) for the DMT-ADSL, a discrete multi-wavelet transform (DMWT) model is proposed. The performance of standard and proposed models is simulated using Matlab software under the additive white Gaussian noise (AWGN) channel effect. The effect of impulse random bit location noise was also taken into our simulation. The simulation results show that the proposed model based on DMWT technique outperforms the standard model in terms of BER.

**Keywords.** DMT, ADSL, AWGN, FFT, DMWT, impulse noise.

---

## 1. Introduction

The multicarrier modulation (MCM) is a favorable choice over single carrier modulation in wide-band communications with frequency selectivity in transmission bands. MCM techniques such as orthogonal frequency division multiplexing (OFDM) and

---

Received September 3, 2011; accepted November 9, 2011.

<sup>†</sup>Türkçe özet ve anahtar kelimeler, orijinal İngilizce metindeki ilgili kısmın doğrudan tercümesi olup *Çankaya University Journal of Science and Engineering* editörlüğü tarafından yazılmıştır. | Turkish abstract and the keywords are written by the editorial staff of *Çankaya University Journal of Science and Engineering* which are the direct translations of the related original English text.

discrete multi-tone (DMT) modulation have been receiving increasing attention in the literature, and have been incorporated into numerous standards. MCM divides a transmission band into orthogonal subchannels. In a wire line broadband communication system, some frequency discontinuities of transmission band normally exist due to various line impairments. MCM is attractive due to the ease with which it can combat channel dispersion without implementation of sharp band-stop filters as in the case of single carrier transmission. In broadband wireline communications, DMT modulation is standardized for asymmetric digital subscriber line (ADSL) and very-high-speed digital subscriber line (VDSL) modems. Maximizing the bit rate is the ultimate goal for such systems [1]. DMT partitions a broadband channel into a large number of virtually independent, narrowband subchannels. Ideally, each narrowband subchannel would have a flat frequency response and could be modeled as a gain plus additive white Gaussian noise (AWGN). The total number of bits transmitted over the broadband channel would be the sum of the bits transmitted in each narrowband subchannel [2].

The orthogonality of subchannels can be obtained by using the FFT algorithm (IFFT at the transmitter side and FFT at the receiver side). A spectrally shaped channel, however, destroys the orthogonality between subchannels so that they cannot be fully separated at the receiver and causes both intercarrier interference (ICI) and inter-symbol interference (ISI) [2, 3]. One solution to prevent ISI is to add an appropriately long guard period at the beginning of each DMT symbol. When the guard period is a cyclic prefix, that is, a copy of the last  $v$  samples of a DMT symbol, ICI can be reduced. For highly dispersive channels, the length of the cyclic prefix is large resulting in an appreciable bit rate loss, especially for a moderate size FFT.

In 1993, Yee *et al.* [5] examined a novel digital modulation/multiple access technique called multi carrier-code division multiple access (MC-CDMA) where each data symbol is transmitted at multiple narrowband subcarriers. Each subcarrier is encoded with a phase offset of 0 or  $p$  based on a spreading code. Analytical results are presented on the performance of this modulation scheme in an indoor wireless multipath radio channel. Negash and Nikookar [6], replaced the conventional Fourier based complex exponential carriers of the OFDM system with some orthonormal wavelets in order to reduce the level of interference. The wavelets are derived from multistage tree-structured Haar and Daubechies orthonormal quadrature mirror filter (QMF) bank. As compared with the conventional OFDM, it

is found that the Haar and Daubechies-based orthonormal wavelets are capable of reducing the power of ISI and ICI.

Tai-Chiu Hsung *et al.* [7] suggested a new discrete multi-wavelet transform (DMWT) structure in which the prefilter is combined with the first stage of DMWT. The advantages of this structure are: The first is the reduction in the computational complexity because the prefiltering stage is embedded into DMWT. The second is the new structure which provides additional design freedom that allows the resulting prefilters to be maximally decimated, orthogonal, symmetric and low multiplicity for multiwavelets coefficients.

Zheng Wu and Chen Jianxun [8] have introduced a method of image noise reduction based on multiwavelet transform and data fusion. In this method, several images, including the same original signal and noises are decomposed by wavelet transform. In a high frequency area, the coefficients are processed by a threshold operation, and then important wavelet coefficients are selected according to multiscale data fusion. In low frequency, the new approximation coefficients are obtained directly by the weighted mean value of the coefficients in different images. In addition, the fused image can be obtained by using the inverse multiwavelet transform for all important coefficients and approximation coefficients. Experimental results show that, image noise can be reduced effectively by using this method and little image detail is lost.

G. S. Tombras *et al.* [9] proposed alternative structure for MC-CDMA based on DMWT. After testing their new structure, they concluded that it gives less bit error rate (BER) performance than the conventional MC-CDMA that employs the FFT or wavelet transform (WT) in its structure. They tested the new structure in different models of channel, namely; AWGN, flat fading and selective fading. The simulation results showed that the new structure outperforms the other two schemes in the performed tests for AWGN, flat fading and selective fading channels.

In this paper, we propose a new structure of DMT-ADSL based on the multiwavelet transforms and we perform a comparison of the new structure with the conventional systems based on FFT. Also, the effect of channel model, (AWGN and AWGN with impulse noise) will be considered in Section 5.

## 2. Discrete Multi-Tone Modulation

DMT partitions a data transmission channel with ISI into a set of orthogonal, memoryless subchannels, each with its own “carrier” [10]. Data is transmitted through

each subchannel independently of other subchannels. Previous research has shown that such a system is capable of transmitting at the highest data rate when allocating more bits and powers to subchannels with higher signal-to-noise ratio (SNR) [11, 12]. DMT modulation is one of many multicarrier techniques including vector coding, structured channel signaling, and discrete wavelet multi-tone modulation. The characteristics of the ADSL signals are defined in the ITU-T Rec. G.992.1 standard. The ADSL line code is the discrete multi-tone (DMT) code. Discrete Fourier transform (DFT) techniques are used to decompose the modulated signal into many mutually orthogonal signals, located at a spacing of 4.3125 kHz (in accordance with the ITU-T Rec. G.992.1 standard, the downstream signal is decomposed into 256 discrete subcarriers, and the upstream signal into 32 subcarriers). Each sub-channel has been allocated bits in the range of 1-15 bits/symbol/Hz, and the symbol time is 250  $\mu$ sec [32]. The assignment of the number of bits for each subchannel, in the form of a *bit allocation table*, is exchanged between the transmitter and the receiver during *initialization* and *retraining* [13].

Figure 1 illustrates a DMT based transceiver along with the channel. In a DMT based transceiver, a bit stream is encoded/decoded into a set of quadrature amplitude modulation (QAM) symbols, called *sub-symbols*. Each sub-symbol is a complex number that carries the number of bits determined by the bit allocation table in one subcarrier. DMT modulation and demodulation are implemented using the inverse discrete Fourier transform (IDFT) and discrete Fourier transform (DFT), respectively. To implement an  $N/2$  subchannel DMT system, an  $N$  size IDFT/DFT is required. The size is doubled by mirroring the data to impose conjugate symmetry in the frequency domain, which results in real-valued signal in the time domain after applying the IDFT. The IDFT and DFT are implemented very efficiently using the well known inverse fast Fourier transform (IFFT) and fast Fourier transform (FFT) algorithms. The other functionalities of the ADSL transceiver also include serial-to-parallel/parallel-to-serial conversion, cyclic extension, digital-to-analog/analog-to-digital conversion, time-domain equalization (TEQ), and frequency-domain equalization (FEQ). A  $T$ -tap pre-filter TEQ, is implemented if the channel duration is too long compared to the length of the cyclic extension [9]. TEQ suppresses the radio frequency interference from amateur radio bands, while FEQ compensates for magnitude and phase distortion caused by the channel and the TEQ [13].

The total number of bits encoded/decoded by the QAM encoder/decoder bank is fixed since our implementation does not retrain and dynamically update the bit

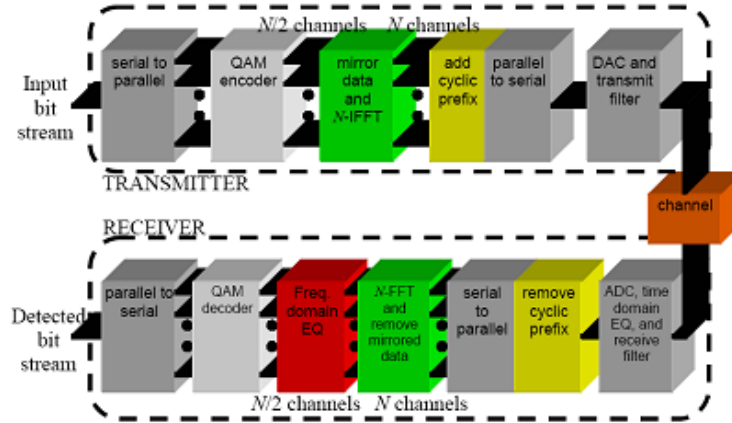


FIGURE 1. A block diagram for data transmission on an ADSL transceiver based on FFT [13, 14].

allocation table. Each QAM encoder/decoder encodes/decodes a number of bits determined by the bit allocation table. The number of QAM encoders/decoders in the QAM bank is equal to the number of subcarriers used by the system. Figure 2 shows the synchronous dataflow locks for an individual QAM encoder/decoder.

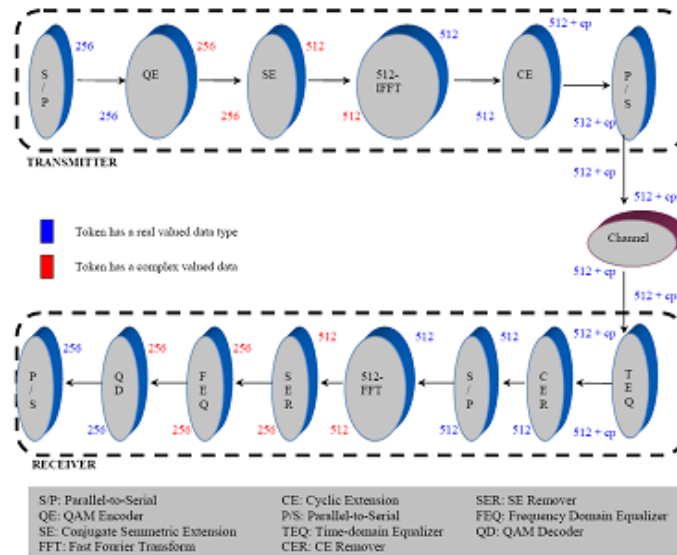


FIGURE 2. Synchronous dataflow model for the discretized ADSL transceiver that uses 256 subcarriers [13].

### 3. Proposed Model Based on DMWT

Multiwavelet transform was introduced previously and found wide spread application in several fields due to the orthogonally of basis functions and their greater suitability for use in communication systems. This high degree of suitability is related to the finite support and self-similarity of the basis functions. The replacement of the fast Fourier transform (FFT) by the multiwavelet transforms leads to overcoming several limitations and improves performance efficiency [9]. The Haar-based orthonormal wavelets are capable of reducing the ISI and ICI, which are caused by the loss in orthogonality between the carriers. The proposed model based on multifilters is called multiwavelets. A very important multiwavelet filter is the GHM filter proposed by Geronimo, Hardian, and Massopust. The GHM basis offers a combination of orthogonality, symmetry, and compact support, which cannot be achieved by any scalar wavelet basis. The GHM will be used in the DMT system. In multiwavelets setting, GHM multiscaling and multiwavelets function coefficients are  $2 \times 2$  matrices, and during transformation step they must multiply vectors (instead of scalars) [15, 16]. This means that multifilter bank needs 2 input rows. The aim of preprocessing is to associate the given scalar input signal of length  $N$  to a sequence of length-2 vectors in order to start the analysis algorithm, and to reduce the noise effects. In the one dimensional signals, the “repeated row” scheme is convenient and powerful to implement. The block diagram of the proposed system for DMT-ADSL based on DMWT is shown in Figure 3. The processes of the S/P converter, the signal mapper and the cyclic prefix are the same as in the system of DMT-ADSL based on FFT. After that a computation of IDMWT for 1-D signal is achieved. By using an over-sampled scheme of preprocessing (repeated row), the inverse discrete multiwavelet transform (IDMWT) matrix is doubled in dimension compared with that of the input, which should be a square matrix  $N \times N$  where  $N$  must be power of 2. Transformation matrix dimensions have equal input signal dimensions after preprocessing. Scaling functions and orthogonal wavelets are created from the coefficients of a low pass and high pass filter (in a two-band orthogonal filter bank). For “multifilters”, those coefficients are matrices. This gives a new block structure for the filter bank, and leads to multiple scaling functions and wavelets. Geronimo, Hardin, and Massopust constructed two scaling functions that have extra properties which were not previously achieved [16-18]. The functions  $\phi_1$  and  $\phi_2$  are symmetric, their scaling functions are orthogonal, including fast processing algorithms, and perfect reconstruction precision.

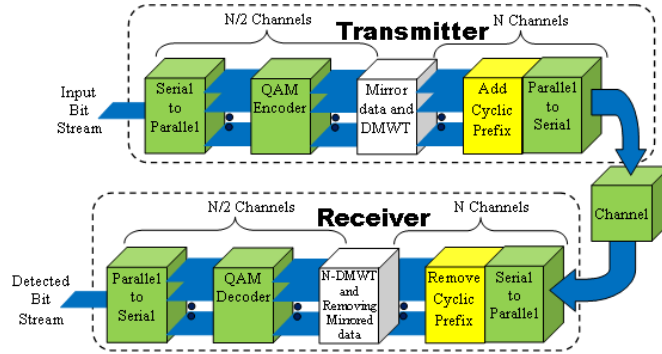


FIGURE 3. A block diagram for data transmission in the proposed DMT-ADSL transceiver based on DMWT.

For notational convenience, the set of scaling functions can be written by using the notation

$$\Phi(t) = \left[ \begin{matrix} \phi_1(t) & \phi_2(t) & \cdots & \phi_r(t) \end{matrix} \right]^t \tag{1}$$

where  $\Phi(t)$  is called the multiscaling function. Likewise, the multiwavelets function is defined from the set of wavelet functions as

$$\Psi(t) = \left[ \begin{matrix} \psi_1(t) & \psi_2(t) & \cdots & \psi_r(t) \end{matrix} \right]^t \tag{2}$$

When  $r = 1$ ,  $\Psi(t)$  is called a scalar wavelet, or simply wavelet. While in principle,  $r$  can be arbitrarily large, the multiwavelets studied to date are primary for  $r = 2$ . The wavelet two-scaled below equations has nearly identical multiwavelet equivalents [18].

$$\Phi(t) = \sqrt{m} \sum_{k=k_0}^{k_1} H_k \Phi(mt - k) \tag{3}$$

$$\Psi(t) = \sqrt{m} \sum_{k=l_0}^{l_1} G_k \Phi(mt - k) \tag{4}$$

Note, however, that  $H_k$  and  $G_k$  are matrix filters, that is,  $H_k$  and  $G_k$  are  $m \times m$  matrices for each integer  $k$ . The matrix elements in these filters provide more degrees of freedom than a traditional scalar wavelet. These extra degrees of freedom can be used to incorporate useful properties into the multiwavelets filters, such as orthogonality, symmetry and high order of approximation. However, the multi-channel nature of multiwavelets also means that the sub band structure resulting from passing a signal through a multifilter bank is different.

The two-scale equations in (3) and the two wavelet equations in (4) can be realized as a matrix filter bank operating on  $m$  input data stream and filtering them into  $2m$  output data streams, each of which is down sampled by factor 2. In the scalar-valued expression  $v_{j,k}^l$ ,  $j$  refers to the scale,  $k$  refers to the translation, and  $l$  refers to the sub-channel or vector row. The equations are:

$$v_{j-1,k} = \sum_m H(m - 2k)v_{j-1,k} \quad (5)$$

$$w_{j-1,k} = \sum_m G(m - 2k)v_{j-1,k} \quad (6)$$

**3.1. Choice of multi-filter.** The standard notation for the case  $m = 2$  is to use  $\phi$ ,  $\psi$  for the scaling and wavelet function. A very important multiwavelet system was constructed by Donovan-Geronimo-Hardian-Massopust (DGHM) [20]. Their system contains the two scaling functions  $\phi_1(t)$ ,  $\phi_2(t)$  and the two dual wavelets  $\psi_1(t)$ ,  $\psi_2(t)$  shown in Figure 4.

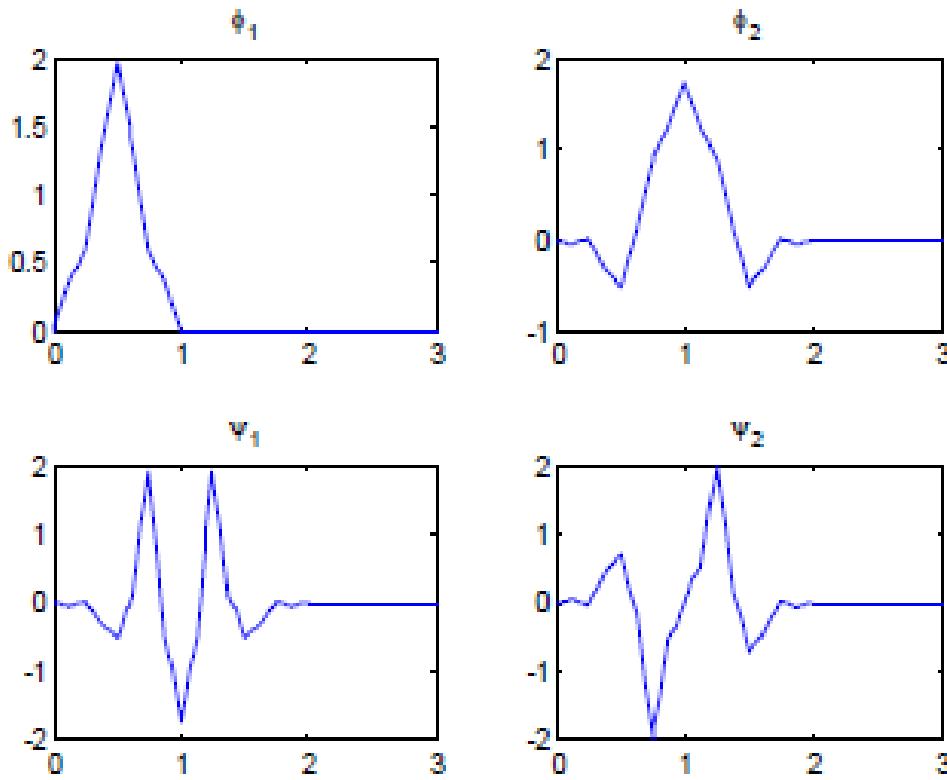


FIGURE 4. The two components of the DGHM refinable function vectors  $(\phi_1, \phi_2)$  and the dual wavelet functions  $(\psi_1, \psi_2)$ .



According to (3) and (4), the GHM two scaling and wavelet functions satisfy the following two-scale dilation equations [16, 19, 20]:

$$\begin{bmatrix} \phi_1(t) \\ \phi_2(t) \end{bmatrix} = \sqrt{m} \sum_k H_k \begin{bmatrix} \phi_1(mt - k) \\ \phi_2(mt - k) \end{bmatrix} \tag{7}$$

$$\begin{bmatrix} \psi_1(t) \\ \psi_2(t) \end{bmatrix} = \sqrt{m} \sum_k G_k \begin{bmatrix} \psi_1(mt - k) \\ \psi_2(mt - k) \end{bmatrix} \tag{8}$$

The signal level of one-dimensional discrete multiwavelet transform can be computed by the next steps:

1. The input vector should be of length  $N$ , where  $N$  must be power of 2, for example, 8, 16, 32, 64, 128, 256 and so on.
2. Construct the transformation matrix TM, using DGHM low and high pass filters matrices given in (3) and (4), the TM can be written as in (9). After the substitution of DGHM matrix, a  $2N \times 2N$  transformation matrix results. For computing discrete multiwavelet transform, scalar wavelet transform matrices (5) and (6) can be written as in the next equation at  $m = 2$ :

$$W = \begin{bmatrix} H_0 & H_1 & H_2 & H_3 & 0 & 0 & \dots & 0 & 0 & 0 & 0 \\ 0 & 0 & H_0 & H_1 & H_2 & H_3 & \dots & 0 & 0 & 0 & 0 \\ \vdots & \vdots & \vdots & \vdots & \vdots & \vdots & \ddots & \vdots & \vdots & \vdots & \vdots \\ H_2 & H_3 & 0 & 0 & 0 & 0 & \dots & 0 & 0 & H_0 & H_1 \\ G_0 & G_1 & G_2 & G_3 & 0 & 0 & \dots & 0 & 0 & 0 & 0 \\ 0 & 0 & G_0 & G_1 & G_2 & G_3 & \dots & 0 & 0 & 0 & 0 \\ \vdots & \vdots & \vdots & \vdots & \vdots & \vdots & \ddots & \vdots & \vdots & \vdots & \vdots \\ 0 & 0 & 0 & 0 & 0 & 0 & \dots & G_0 & G_1 & G_2 & G_3 \\ G_2 & G_3 & 0 & 0 & 0 & 0 & \dots & 0 & 0 & G_0 & G_1 \end{bmatrix} \tag{9}$$

The low and high-pass filter impulse responses are  $H_i$  and  $G_i$  respectively, with dimensions of  $2 \times 2$ .

3. The preprocessing step can be applied on the input signal by repeating the input stream multiplied by a constant value  $= 1/\sqrt{2}$  for DGHM system. The DGHM multiscaling function is commonly considered to be the first nontrivial example of multiscaling function (the upper part of Figure 2). It has recursion

coefficients:

$$H_0 = \frac{1}{20\sqrt{2}} \begin{bmatrix} 12 & 16\sqrt{2} \\ -\sqrt{2} & -6 \end{bmatrix} \quad H_1 = \frac{1}{20\sqrt{2}} \begin{bmatrix} 12 & 0 \\ 9\sqrt{2} & 20 \end{bmatrix} \quad (10)$$

$$H_2 = \frac{1}{20\sqrt{2}} \begin{bmatrix} 0 & 0 \\ 9\sqrt{2} & -6 \end{bmatrix} \quad H_3 = \frac{1}{20\sqrt{2}} \begin{bmatrix} 0 & 0 \\ -\sqrt{2} & 0 \end{bmatrix}$$

While the wavelet matrices  $G_0$ ,  $G_1$ ,  $G_2$  and  $G_3$  of DGHM are:

$$G_0 = \frac{1}{20\sqrt{2}} \begin{bmatrix} -\sqrt{2} & -6 \\ 2 & 6\sqrt{2} \end{bmatrix} \quad G_1 = \frac{1}{20\sqrt{2}} \begin{bmatrix} 9\sqrt{2} & -20 \\ -18 & 0 \end{bmatrix} \quad (11)$$

$$G_2 = \frac{1}{20\sqrt{2}} \begin{bmatrix} 9\sqrt{2} & -6 \\ 18 & -6\sqrt{2} \end{bmatrix} \quad G_3 = \frac{1}{20\sqrt{2}} \begin{bmatrix} -\sqrt{2} & 0 \\ -2 & 0 \end{bmatrix}$$

**3.2. Preprocessing and postprocessing.** The low and high pass filters consist of coefficients corresponding with the dilation (7) and wavelet (8). But in the Multiwavelet setting these coefficients are  $m$  by  $m$  matrices, and during the convolution step, they must multiply vectors (instead of scalars). This means that multifilter banks need  $m$  input rows. In the present case,  $m = 2$ , this means two data streams can enter the multifilter bank at the same time.

The preprocessing step is used to formalize the size of input data to be of length  $N$ , where  $N$  is the vector size of data which corresponds to the frequency bin in the FFT system used in DMT-ADSL or OFDM. In this case, the input data ( $D$ ) of length-2 vectors are formed from the original time series according to the following equation [9, 16].

$$D_{1,N} = \begin{bmatrix} D_{1,k} & D_{1,k+1} \end{bmatrix} = \begin{bmatrix} X_{1,k} & \frac{1}{\sqrt{2}}X_{1,k} \end{bmatrix}, \quad k = 0, 1, \dots, \left(\frac{N}{2} - 1\right). \quad (12)$$

As in (10) the repeated row preprocessing doubles the number of input data points from  $N/2$  to  $N$ . The output data vector after preprocessing step can be obtained by the next equation. Note that the preprocessing step will not increase the transmitted signal power because the data are multiplied by a factor less than 1 (that is,  $1/\sqrt{2}$ ).

$$\begin{bmatrix} 1 & 0 & 0 & \dots \\ \frac{1}{\sqrt{2}} & 0 & 0 & \dots \\ 0 & 1 & 0 & \dots \\ 0 & \frac{1}{\sqrt{2}} & 0 & \dots \\ 0 & 0 & 1 & \dots \\ \vdots & \vdots & \vdots & \ddots \end{bmatrix} \begin{bmatrix} X_0 \\ X_1 \\ X_2 \\ X_3 \\ \vdots \end{bmatrix} = \begin{bmatrix} X_0 \\ \frac{1}{\sqrt{2}}X_0 \\ X_1 \\ \frac{1}{\sqrt{2}}X_1 \\ \vdots \end{bmatrix} = \begin{bmatrix} v_{0,0}^0 \\ v_{0,0}^1 \\ v_{0,1}^0 \\ v_{0,1}^1 \\ \vdots \end{bmatrix} \quad (13)$$

After the inverse of DMWT block at the receiver side, we should remove the repeated data in the transmitter side at the preprocessing step, and this can be done by removing the repeated data according to its locations at the transmitter side.

#### 4. Impulse Noise

In recent years, digital subscriber line (DSL) technology has been gaining popularity as a high speed network access technology, capable of the delivery of multimedia services. A major impairment for DSL is impulse noise in the telephone line. However, evaluating the data errors caused by this noise is not trivial due to its complex statistical nature, which until recently had not been well understood, and the complicated error mitigation and framing techniques used in DSL systems. The impulse noise is characterized statistically through its amplitudes, duration, inter-arrival times, and frequency spectrum, using the British Telecom/University of Edinburgh/Deutsche Telekom (BT/UE/DT) model [4]. This model is broadband, considers both the time and the frequency domains, and accounts for the impulse clustering. It is based on recent measurements in two different telephone networks (the UK and Germany) and therefore is the most complete model available to date and suited for DSL analysis. Impulse noise is a non-stationary stochastic electromagnetic interference which consists of random occurrences of energy spikes with random amplitude and spectral content. The causes of impulse noise on the telephone line are diverse and vary from telephone on/off-hook events, through noise from home, office, and industrial electrical appliances, and transport vehicles, to atmospheric noise from electrical discharges. The resulting interference into the telephone twisted pairs is a major impairment for DSL systems. It is therefore essential to know the statistical nature of impulse noise in order to be able to evaluate its impact on transmission technologies. In the time domain, impulse noise is characterized with the impulse

voltage amplitudes, impulse durations, and inter-arrival times. The impulse amplitude model is based on an approach originally proposed by Henkel and Kessler in [21-23], which consists of approximating the voltage histograms with a generalized exponential distribution of the form [4]:

$$f_{ge}(u) = \frac{1}{240u_0} e^{-|u/u_0|^{1/5}} \quad (14)$$

where  $u$  is the voltage and  $u_0$  is a scaling parameter. This model reflects well the fact that voltage distributions are heavy-tailed [27] and offers a good approximation for all measured impulse noise voltage amplitude distributions collected in the networks [21-25]. Nevertheless, a Weibull density has also been investigated as a possible alternative in [25] because it is mathematically more tractable when using the results of Tough and Ward [28] to generate random noise with prescribed amplitude and spectral characteristics. In the statistics literature the Weibull density function is defined as [4, 26]:

$$f_{wb}(y) = \begin{cases} \alpha b \times u^{\alpha-1} \times e^{-by^\alpha} & \text{if } y \geq 0 \\ 0 & \text{elsewhere} \end{cases} \quad (15)$$

Equation (15) has been modified in [25] to a double Weibull density to make it symmetrical:

$$f_{wb}(y) = \frac{1}{2} \alpha b |u|^{\alpha-1} e^{-b|u|^\alpha} \quad (16)$$

where  $\alpha > 0$  and  $b > 0$  are shape parameters. References [4, 25] explained the details of impulse noise power. In the case of the Germany telecommunication data, the fact that three frequency components were involved required a slightly different approach. Essentially, the width of the peaks in the frequency domain was used via Fourier transform theory to relate the decay rate for each of the individual components. While the exponential decay histograms was well modeled using a straightforward Gaussian pdf in the case of the British Telecommunication data. Table 1 summaries the definitions of the four impulse length bins [25].

TABLE 1. Definition of four impulse length bins.

| <b>Bin name</b> | <b>Bin length (<math>\mu\text{s}</math>)</b> |
|-----------------|--|
| shortest        | 0-1  |
| short           | 1-3  |
| medium          | 3-10   |
| long            | >10  |

## 5. Simulation Results

In this section, the performance of the proposed and the conventional models will be studied under the AWGN channel characteristics. The simulation parameters are given in Table 2 [4, 29-31].

TABLE 2. Simulation parameters for DMT-ADSL.

|                                  |           |
|----------------------------------|-----------|
| Modulation Type=QAM              | 64-QAM    |
| Number of effective sub-carriers | 128, 256  |
| Data rate                        | 6.536Mbps |
| Channel model                    | AWGN      |

**5.1. The performance at the AWGN channel.** The simulation performance of both models (standard and proposed DMT-ADSL) is simulated without taking the equalization into consideration (for simplicity purposes). The data length of the proposed model based on DMWT will be of length 128 bit (with and without mirroring them). The channel is modelled as an additive white Gaussian noise (AWGN) for wide range of SNR from 0 dB to 40 dB; the results are shown in Figure 5. From this figure, it is found that the proposed model of DMT-ADSL based on DMWT technique has a BER= $10^{-4}$  at SNR=13.5 dB, while the conventional model has high BER in the AWGN channel (35.5 dB). So, the proposed model has less BER and more significant than the conventional system based on the FFT transform. The obtained gain is about 22 dB, and one may ask why such wide gain is obtained from the proposed model relative to the conventional system based FFT. To answer this question let us return back to the output signal from the IFFT processor at the transmitter side, even we mirrored the data to eliminate the imaginary part of the transmitted signal but the signal power at the output of IFFT is divided by  $N$  as given in the next equation [31]:

$$X_p(n) = \frac{1}{N} \sum_{k=0}^{N-1} X_p(k) \exp\left(j \frac{2\pi}{N} kn\right), \quad n = 0, 1, \dots, N-1, \quad (17)$$

where  $p$  is the number of symbols and  $N$  is the total vector length of data after mirroring it (that is, after the IFFT block). This means that the power of the modulated symbols (QAM modulator) will reduce after applying the IFFT processing step and leads a reduction of BER performance. In reverse way the use of DMWT has less effect on the signal power than IFFT processor, and this leads to improve the BER performance in addition to the other properties of DMWT mentioned in Section 3.

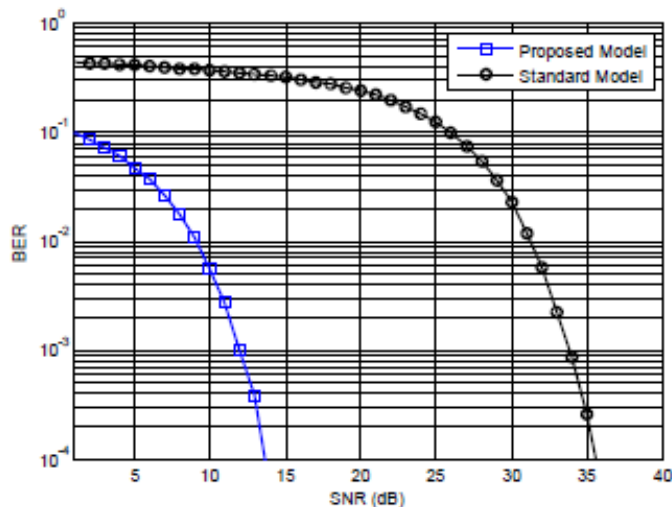


FIGURE 5. Performance of the standard and proposed DMT-ADSL at the AWNG channel (data length  $N = 256$  for DMT-FFT and  $N = 128$  for DMT-DMWT).

**5.2. The performance under the impulse noise effect.** The performance of both models now can be tested under the effect of impulse noise power with and without AWGN channel. Firstly, we test their performance under impulse noise effect alone. From Table 1 the duration of impulse signal started from  $1\mu\text{sec}$ ,  $3\mu\text{sec}$ ,  $10\mu\text{sec}$ , and more than  $10\mu\text{sec}$ . The bit duration in our simulation as in Table 2 is  $15.3\mu\text{sec}$ , we choose the worst case impulse duration which is more than  $10\mu\text{sec}$ .

1. Case 1: Let us consider the impulse duration occupies one bit and that infected bit varies from frame to frame (that is, different bits can be infected in different time), also it is assumed that the amplitude of impulse noise is constant over the time for simulation purposes. The maximum amplitude is twice the maximum signal power.
2. Case 2: Impulse bit duration is ten times the data bit duration with fixed amplitude of impulse noise as in Case 1.
3. Case 3: Repeat Case 1 with AWGN channel.
4. Case 4: Repeat Case 2 with AWGN channel.

### The results.

1. Case 1: After running the simulation program, the standard model has BER of 0.3 which is about 7650 bits out of 25500 transmitted bits, while the proposed model based on DMWT has a BER of 0.0018 which is about 46 bits only.

2. Case 2: The bit error rate for both models is slowly increased.
3. Case 3 and 4: The performance of both models is shown in Figure 6. From this figure, the proposed model has less BER in all range of SNR than standard model based on FFT. As the number of infected bits increased from 1 to 10 bits then the BER also increases (solid line), from this figure the BER for the standard model was not plotted again, because the variation is very small due to high BER in the first curve. After 14 dB the BER in the proposed model based on DMWT is fixed and that is because the maximum amplitude values lie within this range of SNR, so any variation due to the impulse noise can cause errors in the signal. The dotted curve is for DMT-DMWT at  $N = 512$  with mirrored data (that is, the data vector of length 128-bits is preprocessed as given in (13) and it will be of length 256-bits after preprocessing step, then the vector of length 256-bits will be mirrored as in the standard model to get a total vector of length 512-bits). Form this curve (dotted curve) it can be seen that as the vector length increases from 256 to 512 the BER for the proposed model will decrease due to high compression of data via using the DMWT algorithm.

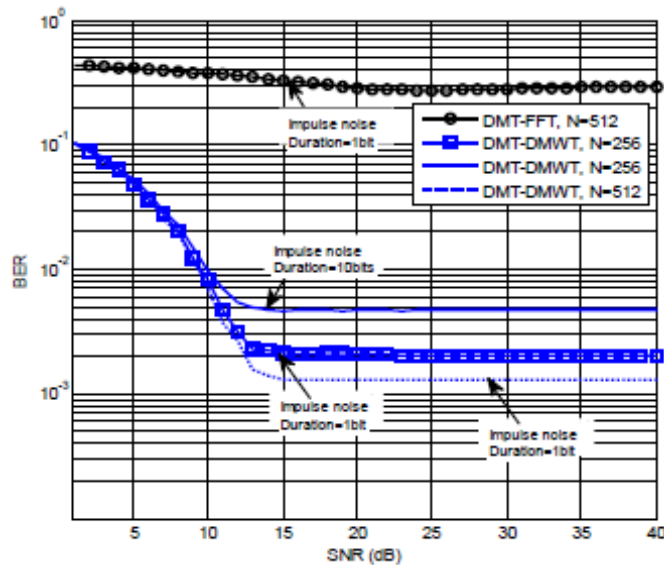


FIGURE 6. Performance of the standard and proposed DMT-ADSL at the AWNG channel and in the presence of impulse noise (data length  $N = 512$  for DMT-FFT and  $N = 256$  and  $512$  for DMT-DMWT).

## 6. Conclusion

An alternative technique based on DMWT was introduced. The new model is important to minimize the BER in the standard DMT-ADSL. The proposed and standard models are simulated using Matlab software. A gain of 22 dB was obtained from the proposed model relative to the standard model at the AWGN channel. In the presence of impulse noise, the BER for both models was increased but the proposed model has less BER than the standard model in all range of SNR. So the proposed model can be considered as an alternative technique to the standard one.

## References

- [1] M. Ding, Z. Shen and B. L. Evans, An achievable performance upper bound for discrete multitone equalization, *IEEE Global Telecommunications Conference (GLOBECOM '04)* **4** (2004), 2297–2301.
- [2] G. Arslan, B. L. Evans and S. Kiaei, Equalization for discrete multitone transceivers to maximize bit rate, *IEEE Transaction on Signal Processing* **49** (2001), 3123–3135.
- [3] J. A. C. Bingham, Multicarrier modulation for data transmission: An idea whose time has come, *IEEE Communications Magazine* **28** (1990), 5–14.
- [4] N. H. Nedev, *Analysis of the Impact of Impulse Noise in Digital Subscriber Line Systems*, Ph.D. Thesis, The University of Edinburgh, Edinburgh 2003.
- [5] N. Yee, J.-P. Linnartz and G. Fettweis, Multi-carrier CDMA in indoor wireless radio networks, *The Fourth International Symposium on Personal, Indoor and Mobile Radio Communications (PIMRC '93)* Yokohama, Japan (1993), 109–113.
- [6] B. G. Negash and H. Nikookar, Wavelet based OFDM for wireless channels, *IEEE VTS 53rd Vehicular Technology Conference* Rhodes, Greece **1** (2001), 688–691.
- [7] T.-C. Hsung, D. Pak-Kong, Y.-H. Shum and K. C. Ho, Generalized discrete multiwavelet transform with embedded orthogonal symmetric prefilter bank, *IEEE Transaction on Signal Processing* **55** (2007), 5619–5629.
- [8] Z. Wu and C. Jianxun, A method of image noise reduction based on multiwavelet transform and multiscale data fusion, *International Symposium on Intelligent Signal Processing and Communication Systems, 2007 (ISPACS 2007)* (2007), 200–203.
- [9] G. S. Tombras, S. M. Salih and A. Mansour, Performance study of MC-CDMA based on multiwavelet transform, *MASAUM Journal of Basic and Applied Sciences* **1** (2009), 138–143.
- [10] P. S. Chow, J. M. Cioffi and J. A. C. Bingham, DMT-based ADSL: concept, architecture, and performance, *IEE Colloquium on High speed Access Technology and Services, Including Video-on-Demand (Digest No. 1994/192)* (1994), 3/1–3/6.
- [11] P. S. Chow, J. M. Cioffi and J. C. Tu, A discrete multitone transceiver system for HDSL applications, *IEEE Journal on Selected Areas in Communications* **9** (1991), 895–908.



- [12] P. S. Chow, J. M. Cioffi and J. A. C. Bingham, A practical discrete multitone transceiver loading algorithm for data transmission over spectrally shaped channels, *IEEE Transactions on Communications* **43** (1995), 773–775.
- [13] E. Erwa, Modeling and simulation of an asynchronous digital subscriber line transceiver data transmission subsystem, <http://users.ece.utexas.edu/~bevans/courses/ee382c/projects/spring04/MustafaErwa/FinalReport.pdf>. Online; accessed 27-October-2011.
- [14] G. Arslan, ADSL Transceivers, Presentation for EE 379K-17 Real-Time Digital Signal Processing Laboratory, The University of Texas at Austin, Austin, TX, November 15, 1999.
- [15] Z. Wu and C. Jianxun, A method of image noise reduction based on multiwavelet transform and multiscale data fusion, *International Symposium on Intelligent Signal Processing and Communication Systems, 2007 (ISPACS 2007)* (2007), 200–203.
- [16] S. N. Abdul-Majeed, *A Multiwavelet Based MC-CDMA System*, Ph.D. Thesis, Baghdad University, Baghdad 2006.
- [17] V. Strela, *Multiwavelets: Theory and Application*, Ph.D. Thesis, Massachusetts Institute of Technology, Cambridge, MA 1996.
- [18] G. Strang and V. Strela, Orthogonal multiwavelets with vanishing moments, *Optical Engineering* **33** (1994), 2104–2107.
- [19] M. Cotronei, L. B. Montefusco and L. Puccio, Multiwavelet analysis and signal processing, *IEEE Transactions on Circuits and Systems II: Analog and Digital Signal Processing* **45** (1998), 970–987.
- [20] G. C. Donavan, J. S. Geronemo, D. P. Hardian and P. R. Massopust, Construction of orthogonal wavelets using fractal interpolation function, *SIAM Journal on Mathematical Analysis* **27** (1996), 1158–1192.
- [21] W. Henkel and T. Kessler, Statistical description and modelling of impulsive noise on the German telephone network, *Electronics Letters* **30** (1994), 935–936.
- [22] W. Henkel and T. Kessler, A wideband impulsive noise survey in the German telephone network: statistical description and modelling, *AEÜ-International Journal of Electronics and Communications* **48** (1994), 277–288.
- [23] W. Henkel, T. Kessler and H. Y. Chung, Coded 64-CAP ADSL in an impulse-noise environment-modelling of impulse noise and first simulation results, *IEEE Journal on Selected Areas in Communications* **13** (1995), 1611–1621.
- [24] W. Henkel and T. Kessler, An impulse-noise model - a proposal for SDSL, Submission to ETSI WG TM6, TD45, 992T45A0, May 1999.
- [25] I. Mann, S. McLaughlin, W. Henkel, R. Kirkby and T. Kessler, Impulse generation with appropriate amplitude, length, inter-arrival, and spectral characteristics, *IEEE Journal on Selected Areas in Communications* **20** (2002), 901–912.
- [26] W. Mendenhall and T. Sincich, *Statistics for Engineering and the Sciences*, Macmillan Publishing, New York 1992.
- [27] S. McLaughlin and D. B. Levey, Statistics of impulse noise: Lengths and energies, Submission to ETSI WG TM6, TD20, 993T20A0, September 1999.

- [28] R. J. A. Tough and K. D. Ward, The correlation properties of gamma and other non-Gaussian processes generated by memoryless nonlinear transformation, *Journal of Physics D: Applied Physics* **32** (1999), 3075–3084.
- [29] J. Kim and E. J. Powers, Subsymbol equalization for discrete multitone systems, *IEEE Transactions on Communications* **53** (2005), 1551–1560.
- [30] M. Barton and M. L. Honig, Optimization of discrete multitone to maintain spectrum compatibility with other transmission systems on twisted copper, *IEEE Journal on Selected Areas in Communications* **13** (1995), 1558–1563.
- [31] K. M. M. Prabhu, A. Madhu Sudana Rao and P. C. W. Sommen, Time-recursive parallel IIR filter structures for the IFFT/FFT in DMT transceiver systems, *Iranian Journal of Electrical and Computer Engineering* **2**(2) (2003), 83–92.
- [32] O. W. Ibraheem and N. N. Khamiss, Design and simulation of asymmetric digital subscriber line (ADSL) modem, *3rd International Conference on Information and Communication Technologies: From Theory to Applications, 2008 (ICTTA 2008)* (2008), 1–6.